

The Role of Dislocations in the Growth of Nanosized Voids in Ductile Failure of Metals

Marc A. Meyers, Sirirat Traiviratana, V.A. Lubarda, David J. Benson, and Eduardo M. Bringa

Dislocations are the most important element in our understanding of the mechanical response of metals. Their postulation in 1934 led to revolutionary advances in our ability to predict the mechanical behavior of materials. The authors recently advanced a dislocation mechanism for void growth in ductile metals. This paper reviews the analytical and atomistic calculations carried out in support of this model. The emission of shear dislocation loops, nucleated at the surface of nanosized voids, is responsible for the outward flux of matter, promoting void growth. This is a new paradigm in the initiation of void growth, which was attributed to convergent vacancy diffusion or to prismatic loops by oth-

ers. The analytical treatment is based on the emission of a dislocation from a void in the plane along which the shear stresses are maximum. Molecular dynamics calculations performed for different orientations of the tensile axis show how the loops generate and expand outward. These loops involve the emission of partial dislocations and are the counterpart for voids of the Ashby geometrically necessary shear loops postulated for rigid particles. This process is demonstrated for bicrystalline and nanocrystalline copper.

INTRODUCTION

Three quarters of a century ago, in 1934, Taylor (in England),¹ Orowan (in Germany),² and Polanyi (in Hungary)³ proposed, almost simultaneously, the concept of the dislocation. There were earlier rumblings, and the idea of Ver-

nier defects (the disregistry that we have all seen in the scale of calipers), closely resembling a dislocation, had already been advanced by Prandtl.^{4,5} Indeed, Seeger⁶ states that Prandtl recognized that the motion of Vernier defects at the interfaces between crystallites could lead to dissipation of mechanical energy. A rudimentary description of the process ("elementare Gleitakt," elementary slip action) was presented by Becker and Orowan⁷ in 1932. Hence, the paternity of dislocations is somewhat muddled. It is also fascinating that a great part of the foundations of dislocation theory was developed prior to experimental verification. From this

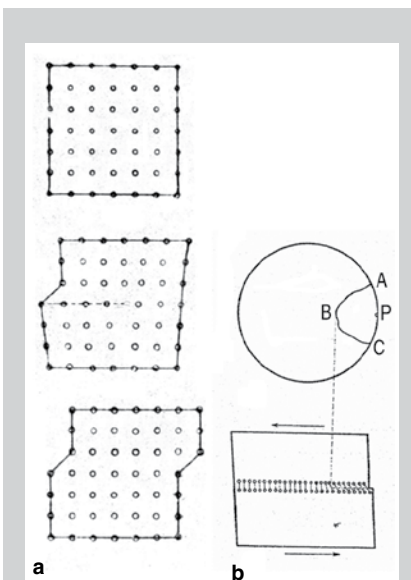


Figure 1. Early representations of dislocations: (a) Taylor's 1934 edge dislocation;¹ the upper image shows the original undistorted lattice, the center image is the lattice with dislocation moving from left to right, and the bottom image shows the sheared lattice; (b) Orowan's dislocation line separating undeformed from slipped material.⁹

How would you...

...describe the overall significance of this paper?

We review some of the seminal contributions to dislocations on the 75th anniversary of their discovery and apply this concept in a new context. We explain how ductile fracture is initiated through the generation of dislocations.

...describe this work to a materials science and engineering professional with no experience in your technical specialty?

We explain how metals fail at the nanoscale. This occurs by the emission of dislocations, the principal agents of plastic deformation in metals.

...describe this work to a layperson?

We identified the processes responsible for the failure of ductile metals at the nanoscale.

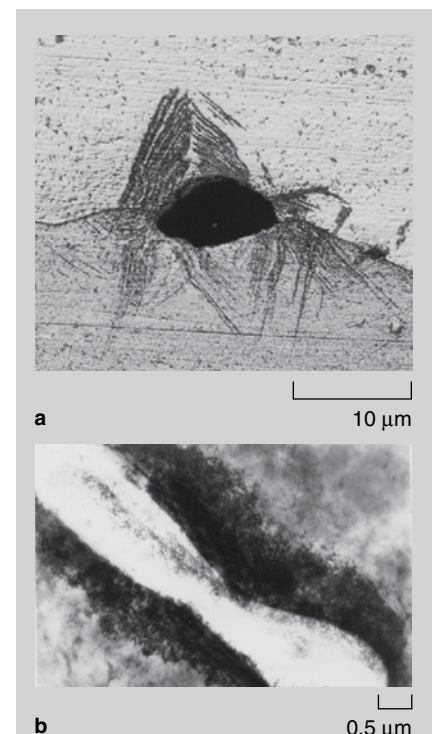
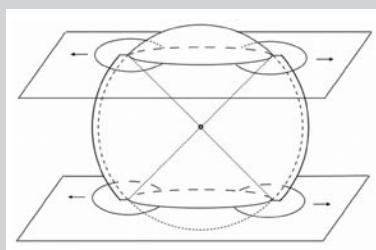
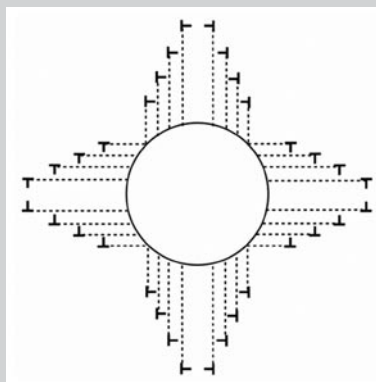


Figure 2. (a) An optical micrograph showing slip bands emanating from a void;⁵⁸ (b) a transmission electron micrograph of peanut-shaped void in copper (region in the spall of a shock compression experiment).⁵⁷

unparalleled exploration of the physical processes in crystalline materials emerged a vast, rigorous, and permanent body of knowledge. Dislocation theory encompasses and explains the principal phenomena in plastic deformation, fracture, fatigue, creep, strengthening mechanisms, temperature and strain rate effects, phase interfaces, and thin films. This has been accomplished by a multitude of scholars, whose works are referenced in Table I, where the most important aspects of dislocation theory are listed. This table is incomplete and



a



b

Figure 3. (a) The emission of four shear loops enabling the expansion of a void; (b) a two-dimensional representation of sequential emission of shear loops as the void grows.³⁷

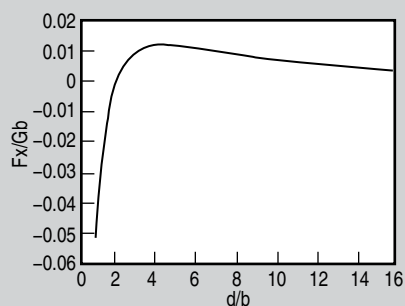


Figure 4. Total normalized force on an edge dislocation situated on the plane of maximum shear under the combined effect of an external tensile traction and image forces due to the free surface of void as a function of normalized distance d/b from void surface.³⁷

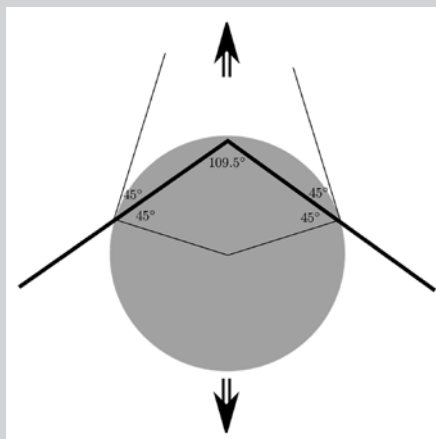
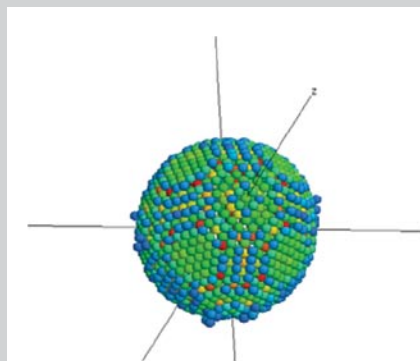
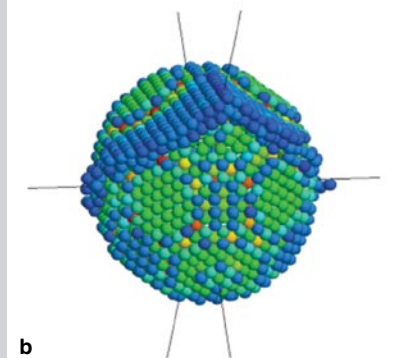


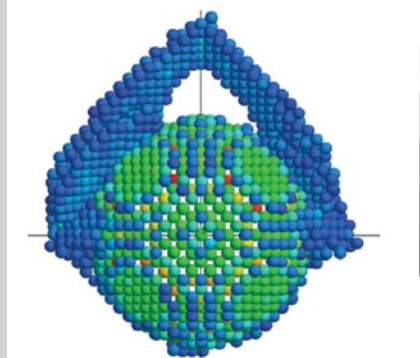
Figure 5. A schematic showing traces of two slip planes intersecting a void at 45° to its surface, where shear stresses are maximum; loading axis $[110]$ marked by arrows.



a



b



c

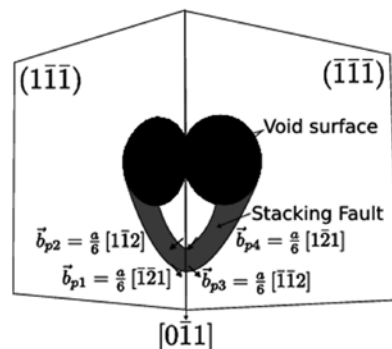
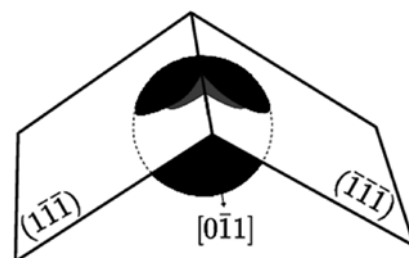
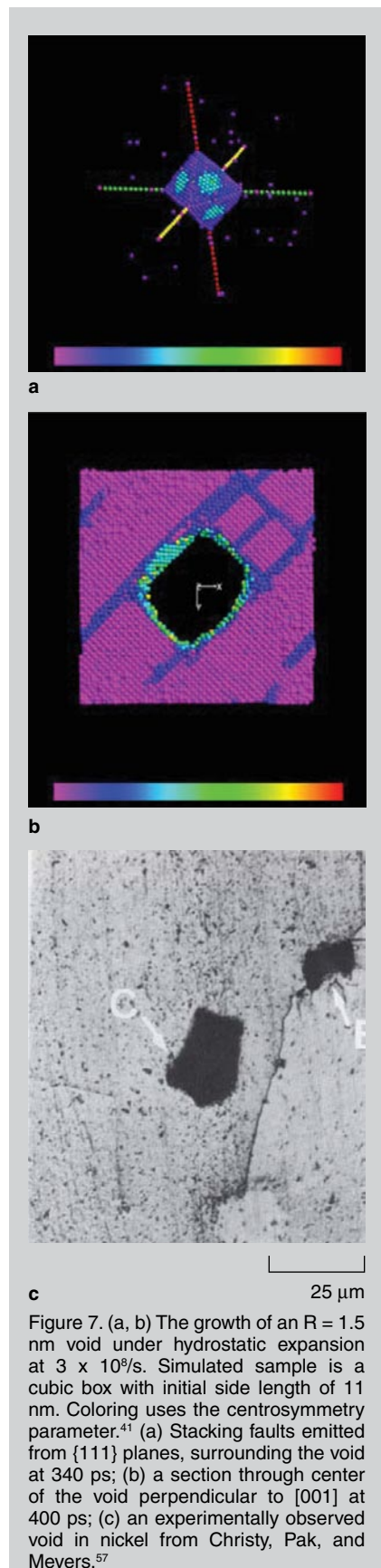


Figure 6. The sequence of shear loop nucleation and growth for $[100]$ loading direction (a) void with 2 nm radius prior to plastic deformation; (b) initiation of partial dislocation emission from (111) and (111) planes; (c) propagation of leading partials and emission of trailing partials with reactions.³⁸ Coloring is based on the centrosymmetry parameter,⁴⁴ with the atoms in the stacking faults in light blue.

is a personal interpretation; nevertheless, the principal cornerstones of dislocation theory are contained therein. Figure 1a shows an edge dislocation as



c 25 μm
 Figure 7. (a, b) The growth of an $R = 1.5$ nm void under hydrostatic expansion at $3 \times 10^8/s$. Simulated sample is a cubic box with initial side length of 11 nm. Coloring uses the centrosymmetry parameter.⁴¹ (a) Stacking faults emitted from {111} planes, surrounding the void at 340 ps; (b) a section through center of the void perpendicular to [001] at 400 ps; (c) an experimentally observed void in nickel from Christy, Pak, and Meyers.⁵⁷

visualized by Taylor in 1934; Figure 1b shows a dislocation line separating the undeformed material from the sheared one as seen by Orowan in 1940.⁹ Both images are remarkable in their simplicity and correctness.

DUCTILE FAILURE

Ductile metals fail by the nucleation, growth, and coalescence of voids, leading to the classical dimpled fracture, in contrast to brittle materials, where fracture is governed by crack nucleation, growth, and coalescence. The nucle-

ation of these voids was one small problem that lay dormant, more by neglect than design: how do voids leading to ductile fracture initiate and grow?

Dislocation motion comes to mind, but the traditional literature contains scant evidence. Seitz²⁷ and Brown²⁸ postulated prismatic loops forming at the interface between a rigid particle and its matrix. In related work, Silcox and Hirsch²⁹ analyzed the dislocations that form the boundaries of stacking-fault tetrahedra in gold. These tetrahedra had sizes of approximately 35 nm.

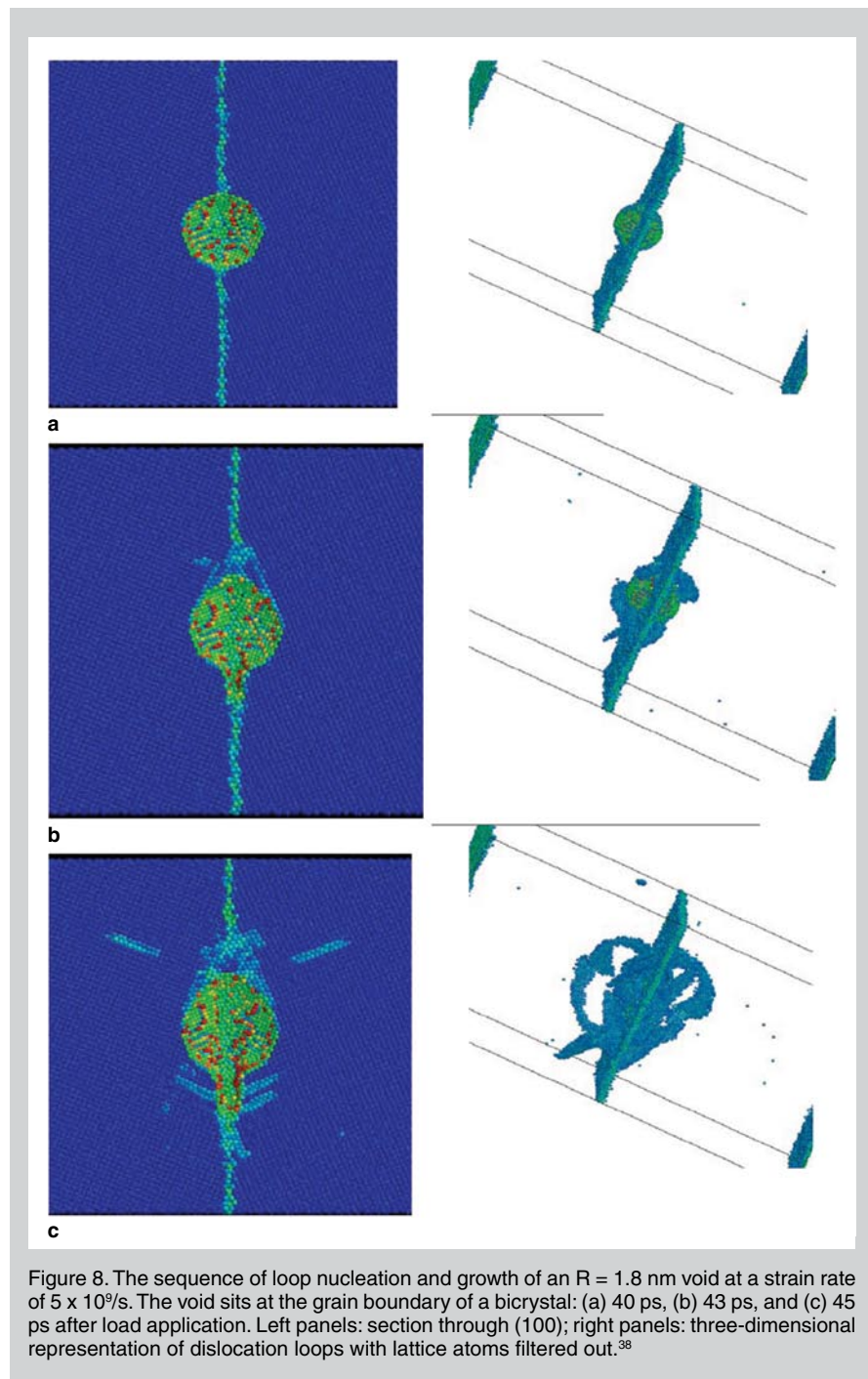


Figure 8. The sequence of loop nucleation and growth of an $R = 1.8$ nm void at a strain rate of $5 \times 10^8/s$. The void sits at the grain boundary of a bicrystal: (a) 40 ps, (b) 43 ps, and (c) 45 ps after load application. Left panels: section through (100); right panels: three-dimensional representation of dislocation loops with lattice atoms filtered out.³⁸

Later, Humphreys and Hirsch³⁰ analyzed copper containing small alumina particles and observed the formation of prismatic loops by a cross-slip mechanism. This study involved primarily the interaction of existing dislocations with rigid particles. More recently, Uberuaga et al.³¹ observed the direct transformation of vacancy voids to stacking fault tetrahedra by molecular dynamics (MD). In the area of initiation and growth of voids under tensile loading, there are only a few dislocation-based mechanisms. One mechanism was proposed by Stevens et al.,³² according to it the void is a sink for dislocations. A second mechanism was proposed by Meyers and Aimone³³ consisting of intersecting dislocations diverging from a point. Both mechanisms are implausible since they are two-dimensional and physically impossible in three dimensions. There is also a vague mention of dislocations in Broek,³⁴ without any specific model being proposed. To treat porosity in radiation-damaged materials, Wolfer⁶⁷ proposed void growth by

emission of prismatic loops, and this mechanism has been adopted by others, like Ahn et al.⁵³ However, since there is a dearth of information on the void initiation process, it was generally assumed that initiation was governed by the diffusion of vacancies toward a central point, creating and nourishing a void. One of the most rapid diffusion mechanisms is “pipe” diffusion, in which vacancies migrate along the dislocation line. Cuitiño and Ortiz³⁵ developed a specific mechanism for this mode, with an equation predicting the time change of void radius in terms of the pipe diffusion coefficient. Failure in ductile metals is typically characterized by voids with radii ranging in the micrometers. Calculations based on pipe diffusion by Cuitiño and Ortiz³⁵ at 300 K show that the time required to reach this size of void is unrealistically long (10^{10} s). Even at 600 K, voids cannot grow to a size equal to $0.1 \mu\text{m}$ in 10^2 s. Thus vacancy diffusion, which is the principal mechanism of void growth in creep fracture, as treated by

Raj and Ashby,³⁶ cannot be the operating mechanism in conventional plastic deformation.

Figure 2a shows a void formed at a grain boundary in copper shock compressed to a pressure of 37 GPa; the shock wave was allowed to reflect at the free surface as a tensile pulse. The etchant reveals a pattern of slip markings that are clear evidence of dislocation activity. Figure 2b shows one of the few transmission electron microscopy (TEM) micrographs of a void from this sample, in this case a peanut-shaped one also generated in the spall region of a copper plate. The void is for the most part contained within the thin foil and was stereoiaged. The high-voltage Kratos TEM, at the National Center for Electron Microscopy, was used at an accelerating voltage of 10^6 V. A dark band surrounding the void can be seen. It is probable that the peanut-shaped void represents the coalescence of two voids. The dark band consists of a region with high dislocation density. However, the voids shown in Figure 2 have a micrometer size scale and represent an advanced growth stage. What happens at the initiation of these voids was unknown until recently.

EMISSION OF LOOPS: ANALYSIS

In 2004, Lubarda et al.³⁷ proposed prismatic and shear loops to accomplish the divergent material flow necessary for void growth. While prismatic loops were already known,⁶⁷ the concept of shear loops was novel. The Lubarda et al. proposal is analogous to the Ashby¹⁹ mechanism for the generation of geometrically necessary dislocations in the deformation of plastically inhomogeneous materials. The emission of shear loops from the void surface, similar to Ashby’s geometrically necessary dislocations, generates densities compatible with experimental observations, as was shown by Traiviratana et al.³⁸ Figure 3a shows the original model of shear loop expansion proposed by Lubarda et al.³⁷ Sequential loops are nucleated farther and farther from the center of the void as it expands (Figure 3b).

The force acting on a dislocation in the vicinity of a void as a balance of the externally applied stress σ (a biaxial

Table I. Seminal Contributions to Dislocation Theory

Researcher	Year	Contribution	Number of Citations*
Prandtl [4, 5]	1913	Vernier defects	
Orowan [2, 7]	1932, 1934	Edge dislocation	
Taylor [1]	1934	Edge dislocation	
Polanyi [3]	1934	Edge dislocation	
Burgers [8]	1939	Screw dislocation	
Orowan [9]	1940	Connection with continuum plasticity	218
Nabarro [17]	1947	Dislocation barriers	432
Frank, van der Merwe [58, 59]	1949, 1963	Dislocations in thin films	1288 +739
Cottrell [16]	1949	Interstitial effects	956
Frank & Read [10]	1950	Dislocation sources	295
Seeger [11]	1954	Thermal activation, kink pairs	147
J. Weertman [14, 15]	1955	Creep, supersonic disl.	408
Hirsch, Horne, Wheelan [12]	1956	TEM	247
Johnson & Gilman [13]	1959	Dislocation dynamics	1073
Kröner [61]	1958	Connection with continuum plasticity	644
Li [26]	1963	Grain boundaries and dislocations	331
Conrad [18]	1964	Rate controlling mechanisms	315
Hirth & Lothe [22]	1968	Synthesis of knowledge	4663 (Google Scholar)
Ashby [19]	1969	GNDs, SSDs	1047
Kocks [20]	1970	Polycrystal plasticity	490
Mughrabi [60]	1978	Dislocations in fatigue	475
Kuhlmann-Wilsdorf [21]	1985	Work hardening	101
Zerilli & Armstrong [23]	1987	Constitutive description	332
Nix [25]	1989	Thin films	1160
J.R. Weertman et al. [65]	1991	Dislocations in nanocrystals	300
Rice [62]	1992	Dislocations in cracks	500
Schiøtz et al. [66]	1998	MD of dislocations/ nanocrystals	498

* Web of Science (accessed November 14, 2008)

stress state was assumed) and attraction to the surface (image force) was calculated³⁷ as shown in Equation 1, where $\xi=x/R$. This normalized force is plotted in Figure 4 against the normalized distance of dislocation loop from the void surface. The radius of the void is R , the Burgers vector of the dislocations is b , the stress is σ , and the shear modulus is G . This enables the calculation of the critical distance from the void surface, d_{cr} at which the force vanishes and the dislocation is in equilibrium, as shown in Equation 2, where ν is Poisson's ratio. In analogy with the analysis by Rice and Thomson,³⁹ the critical stress for dislocation emission was taken from the distance d_{cr} equal to the radius of the dislocation core, $R_0 = pb$. This provides the critical stress for dislocation emission (for both prismatic and shear loops), as shown in Equation 3. It can be seen that this stress is a strong function of void radius, in contrast with the widely used Gurson⁴⁰ model of porosity evolution, which is independent of the void size. The authors note that there are other criteria for dislocation nucleation which could be incorporated into our model.

COMPUTATIONAL METHODS AND RESULTS

Several researchers have simulated void growth using MD.^{45–55} Rudd, Seppälä, and Belak^{45–48} were primarily interested in void growth and did not focus on the dislocations. Potirniche et al.⁵³ used a uniaxial stress configuration which led to necking and did not specifically analyze dislocation activity. Zhu et al.⁵⁴ modeled the process under shock loading and unloading conditions and obtained profuse evidence for shear loop emission. Norman and coworkers^{63,64} have carried out MD simulations on void nucleation and growth as well as spalling. Marian, Knapp, and Ortiz^{49,50} used the quasi-continuum simulation method and were indeed the first to identify shear loops and some of their reactions as the strain increased. However, quasicontinuum calculations perform energy minimization of the system at zero temperature and may give results that differ from MD simulations. Davila et al.⁵⁵ modeled the inverse problem: the collapse of a void.

Equations

$$F_x(\xi) = \sqrt{2}\sigma b \frac{\xi}{(\xi^2 + 1/2)^2} - \frac{Gb}{\pi(1-\nu)R} \frac{b}{(\xi^2 + 1/2)^2} \frac{\xi(\xi^4 + 1/4)}{(\xi^2 - 1/4)} \quad (1)$$

$$d_{cr} = \frac{R}{\sqrt{2}} \left\{ \left[\frac{\sqrt{2}\pi(1-\nu)(\sigma/G)(R/b)+1}{\sqrt{2}\pi(1-\nu)(\sigma/G)(R/b)-1} \right]^{1/4} - 1 \right\} \quad (2)$$

$$\frac{\sigma_{cr}}{G} \geq \frac{b/R}{\sqrt{2}(1-\nu)} \frac{(1+\sqrt{2}pb/R)^4 + 1}{(1+\sqrt{2}pb/R)^4 - 1} \quad (3)$$

The MD simulations presented in Reference 38 were expanded upon by the authors. The Large-scale Atomic/Molecular Massively Parallel Simulator (LAMMPS)⁴¹ code was used to describe face-centered cubic (fcc) copper with the embedded atom method (EAM) potential of Mishin et al.⁴³ The number of atoms was varied from 10^5 to 10^7 , and calculations were performed at the San Diego Super Computer Center. The single-crystal copper domain was a cube wherein an initially spherical void was cut at the center. Periodic boundaries were used in all directions, and the box was expanded uniformly along the [001] direction, providing a uniaxial strain state. All simulations were done at an initial temperature of 150 K and strain rate of 10^8 s^{-1} for times of up to 20 picoseconds, corresponding to 20% strain. Visualization of defects, including stacking faults and dislocations, was conducted with a filter using a centrosymmetry parameter.⁴⁴

The calculations, for voids with 2 nm radius, were performed for loading along [100]. The traces of two (out of the eight with equal Schmid factor) slip planes are illustrated in Figure 5 for a [100] loading direction (marked by arrows). The 45° angles with the surface are marked; the two planes make an angle of 109.47° .

The initial void is shown in Figure 6a. As the stress is increased, loop emission occurs, as postulated by Lubarda et al.,³⁷ at the line corresponding to the intersection of the slip plane making an angle of 45° with the surface of the void, which maximizes the shear stress. This is shown in Figure 6b and c. First, the leading partials form simultaneously on (111) and (111) planes. A biplanar shear loop emerges from the surface of the void. The two

leading partial dislocations advance, moving away from the void. The sketches on the right indicate the planes and dislocations. Then, as the leading partials advance, the trailing partials are emitted (Figure 6c). Again, the diagram on the right shows the dislocations and their Burgers vectors.

For the [100] orientation, one clearly observes a cooperative growth of partial dislocation loops. This mechanism was analyzed in detail by Traiviratana et al.³⁸ The dislocation that is formed by the reaction of the leading partials is cancelled by the one forming with the reaction of the trailing partials. Upon further loading, additional loops form on other planes (not shown here). The voids acquire a geometrical shape due to the cooperative expansion of loops along the {111} planes. Figure 7a shows the early stacking faults on eight planes forming an octahedron. All regular lattice atoms have been filtered out. A section through the void center reveals a rectangular shape (Figure 7b). This is also observed experimentally, but at a much larger scale, as shown in Figure 7c. Ruud, Seppala, and Belak^{45–48} had earlier also predicted the geometry of an expanding void.

When the void is at the boundary between two grains, as is shown in Figure 8, the emission of dislocations in each grain follows the respective crystallography. The configuration of slip is analogous to the experimentally observed void shown in Figure 2a. The boundary in Figure 8 is a symmetric boundary. The bicrystal was constructed by two cubes rotating around a [100] axis by 43.6° . Thus, the boundary makes an angle of 21.8° with each of the grains.

Figure 9 shows a nanocrystalline specimen being subjected to tension in the absence of preexisting voids. Dislo-

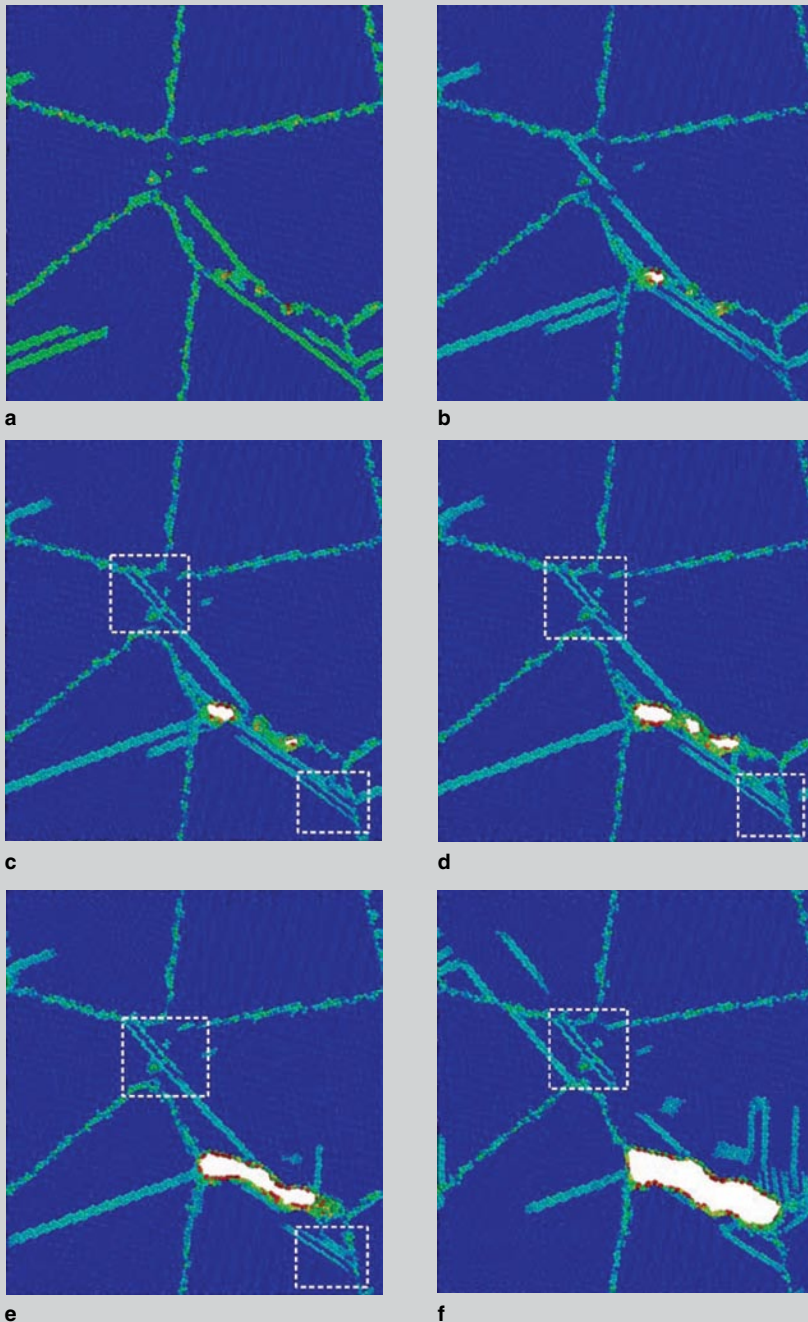


Figure 9. The sequence of (a,b) void nucleation, (c,d) growth, and (e,f) coalescence in nanocrystalline copper under tension. Mean grain size was 5 nm, and strain rate was $10^9/s$. The square boxes indicate twins that are formed during loading, with one of them then disappearing after void coalescence. (a) 620 ps; (b) 675 ps; (c) 690 ps; (d) 710 ps; (e) 730 ps; (f) 775 ps.

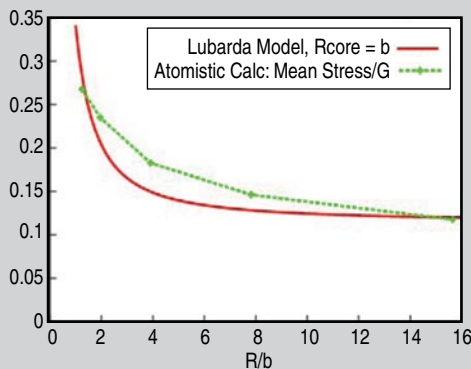


Figure 10. The normalized stress for initiation of plastic deformation as a function of normalized void radius according to analytical calculations by Lubarda et al.³⁷ and the authors' molecular dynamics computations using $G = 48$ GPa and $b = 0.255$ nm (Mischin et al.⁴³). The mean stress in the simulations is given by the pressure, although the stress condition far from the void is not perfectly hydrostatic.

cation emission from the boundaries is seen in Figure 9a. These are partial dislocations similar to the ones seen, for example, by van Swygenhoven et al.,⁵⁶ they completely traverse the boundaries. In Figure 9b nanoscale voids can be seen; they nucleate at grain boundaries. In Figure 9c the number of nanovoids has increased to three, and their growth proceeds by dislocation emission and grain boundary separation in Figure 9d. They eventually coalesce (Figures 9e and f) and would lead to fracture of the sample at larger strains.

COMPARISON OF ANALYSIS AND MD SIMULATIONS

By varying the initial void size in a crystal subjected to tension along [100] it was possible to establish the effect on the nucleation stress. The results are plotted in Figure 10 and compared with the calculated values from Equation 3.³⁷ The Lubarda et al.³⁷ predictions depend on the dislocation core radius and the best match with MD computations is obtained for $R_0 = b$, which is reasonable for dislocations in EAM copper. The model from Lubarda assumes a hydrostatic state far from the void surface, whereas the authors' simulations of uniaxial loading do not match this condition. It should also be noted that the Lubarda model results were found to describe extremely well the critical stress for void collapse from MD simulations of Davila et al.⁵⁵

CONCLUSIONS

Analytical calculations and MD simulations are used to predict the mechanism for the early growth of voids in ductile failure. Void growth proceeds by the cooperative expansion of shear loops that nucleate at the void surface. While the calculations were carried out for a void with 2 nm radius, the same mechanism operates for voids containing as few as 13 vacancies. Thus, it is proposed that homogeneous void initiation in metals takes place at vacancy clusters or special grain-boundary configurations such as triple points through this shear loop expansion mode. Convergent vacancy diffusion is not required for void formation, and the calculations presented here agree with our dislocation-based mechanism for void growth. It should be noted that

none of the MD simulations showed prismatic loops, thought by many to be the primary mechanism for loop expansion.

ACKNOWLEDGEMENTS

Financial support from Lawrence Livermore National Laboratory grant B558558, ILSA contract number W-7405-Eng-48 (program manager: Dr. D. Correll) and National Science Foundation EVO CBET-0742730 program is gratefully acknowledged. We thank Prof. A.S. Argon for elucidating the early contributions by E. Orowan. This paper is dedicated to Prof. H. Mughrabi on his 70th birthday.

References

1. G.I. Taylor, *Proc. Roy. Soc.*, 145 (1934), p. 362.
2. E. Orowan, *Z. Physik*, 89(1934), p. 634.
3. M. Polanyi, *Z. Physik*, 89(1934), p. 660.
4. T. von Karman, *Enzyklopedie der Mathematischen Wissenschaften*, ed. F. Klein and G. Muller, Vol. IV, pt. 4 (Leipzig, Germany: Teubner, 1913), p. 767.
5. L. Prandtl, *Z. Angew. Math. Mech.*, 8 (1928), p. 85.
6. A. Seeger, *Mat. Sci. Eng. A*, 370 (2004), pp. 50–66.
7. R. Becker and E. Orowan, *Z. Physik*, 79 (1932), p. 566.
8. J.M. Burgers, *Proc. Kon. Ned. Akad. Wetenschap.*, 42 (1939), pp. 293, 378.
9. E. Orowan, *Proc. Phys. Soc. (London)*, 52 (1940), p. 8.
10. F.C. Frank and W.T. Read, *Symposium on Plastic Deformation of Crystalline Solids* (Pittsburgh, PA: Carnegie Institute of Technology, 1950), p. 44.
11. A. Seeger, *Z. Naturf.*, 9A (1954), pp. 758, 819, 856.
12. P. Hirsch, R.W. Horne, and M.J. Wheelan, *Phil. Mag.*, 1 (1956), p. 677.
13. W.G. Johnson and J.J. Gilman, *J. Appl. Phys.*, 33 (1959), p. 129.
14. J. Weertman, *J. Appl. Phys.*, 26 (1955), p. 1213.
15. J. Weertman, *J. Appl. Phys.*, 38 (1967), p. 5293.
16. A.H. Cottrell and B.A. Bilby, *Proc. Phys. Soc. (London)*, A62 (1949), p. 49.
17. F.R.N. Nabarro, *Proc. Phys. Soc.*, 59 (1947), p. 256.
18. H. Conrad, *J. Metals*, 16 (1964), p. 582.
19. M.F. Ashby, *Phil. Mag.*, 19 (1969), p. 757.
20. U.F. Kocks, *Met. Trans.*, 1 (1970), pp. 1121–1143.
21. D. Kuhlmann Wilsdorf, *Met. Trans.*, 11A (1985), p. 2091.
22. J.P. Hirth and J. Lothe, *Theory of Dislocations* (New York: McGraw-Hill, 1968).
23. F.J. Zerilli and R.W. Armstrong, *J. Appl. Phys.*, 61 (1987), p. 1816.
24. L.B. Freund, *J. Appl. Mech.*, 54 (1987), pp. 553–557.
25. W.D. Nix, *Met. Trans.*, 20A (1989), pp. 2217–2245.
26. J.C.M. Li, *Trans. Met. Soc. AIME*, 227 (1963), p. 239.
27. F. Seitz, *Phys. Rev.*, 79 (1950), p. 723.
28. L.M. Brown, *Phil. Mag.*, 21 (1970), p. 329.
29. J. Silcox and P.B. Hirsch, *Phil. Mag.*, 4 (1958), p. 72.
30. F.J. Humphreys and P.B. Hirsch, *Proc. Roy. Soc. London*, 318 (1970), pp. 73–92.
31. B.P. Uberuaga et al., *Phys. Rev. Lett.*, 99 (2007), p. 135501.
32. A.L. Stevens, L. Davison, and W.E. Warren, *J. Appl. Phys.*, 43 (1972), p. 4922.
33. M.A. Meyers and C.T. Aimone, *Prog. in Matls. Sci.*, 28 (1983), p. 1.
34. D. Broek, *Elementary Engineering Fracture Mechanics* (Boston, MA: Martinus Nijhoff Publishers, 1986).
35. A.M. Cuitiño and M. Ortiz, *Acta Mater.*, 44 (1996), p. 863.
36. R. Raj and M.F. Ashby, *Acta Metal.*, 23 (1975), p. 653.
37. V.A. Lubarda et al., *Acta Mater.*, 53 (2004), p. 1397.
38. S. Traiviratana et al., *Acta Mater.*, 56 (2008), p. 3874.
39. J.R. Rice and R. Thomson, *Phil. Mag.*, A29 (1974), p. 73.
40. A.L. Gurson, *J. Eng. Mat. Tech.*, 99 (1977), p. 2.
41. S.J. Plimpton, *J. Comp. Phys.*, 117 (1995), p. 1.
42. M.S. Daw and M.I. Baskes, *Phys. Rev. B*, 29 (1984), p. 6443.
43. Y. Mishin et al., *Phys. Rev. B*, 63 (2001), p. 224106-1.
44. C.L. Kelchner, S.J. Plimpton, and J.C. Hamilton, *Phys. Rev. B*, 58 (1998), p. 11085.
45. R.E. Rudd and J.F. Belak, *Comp. Mater. Sci.*, 24 (2002), p. 148.
46. E.T. Seppälä, J.F. Belak, and R.E. Rudd, *Phys. Rev. B*, 69 (2004), p. 134101-1-19.
47. E.T. Seppälä, J. Belak, and R.E. Rudd, *Phys. Rev. Lett.*, 93 (2004), p. 245503-1-4.
48. E.T. Seppälä, J. Belak, and R.E. Rudd, *Phys. Rev. B*, 71 (2005), p. 064112-1-10.
49. J. Marian, J. Knap, and M. Ortiz, *Phys. Rev. Lett.*, 93 (2004), p. 1.
50. J. Marian, J. Knap, and M. Ortiz, *Acta Mater.*, 53 (2005), p. 2893.
51. S.G. Srinivasan, M.I. Baskes, and G.J. Wagner, *J. Mater. Sci.*, 41 (2006), p. 7838.
52. D.C. Ahn et al., *Appl. Phys.*, 101 (2007), p. 063514-1-6.
53. G.P. Potirniche et al., *Int. J. Plasticity*, 22 (2006), p. 257.
54. W. Zhu et al., *Phys. Rev. B*, 75 (2007), p. 024104-1.
55. L.P. Davila et al., *Appl. Phys. Lett.*, 86 (2005), p. 161902.
56. H. van Swygenhoven, M. Spaczer, and A. Caro, *Acta Mat.*, 47 (1999), p. 561.
57. S. Christy, H.-R. Pak, and M.A. Meyers, *Metallurgical Applications of Shock Wave and High-Strain-Rate Phenomena* (New York: Marcel Dekker, 1986), pp. 835–863.
58. F.C. Frank and J.H. van der Merwe, *Proc. Roy. Soc.*, A198 (1949), pp. 205, 216.
59. J.H. van der Merwe, *J. Appl. Phys.*, 34 (1963), pp. 123–127.
60. H. Mughrabi, *Mat. Sci. Eng.*, 33 (1978), p. 207.
61. E. Kröner, *Zeitsch. Fur Physik*, 151 (1958), p. 504.
62. J.R. Rice, *J. Mech. Phys. Sol.*, 40 (1992), p. 239.
63. V.V. Stegailov and A.V. Yanilkin, *Shock Compression of Condensed Matter-2007* (College Park, MD: American Physical Society, 2008), pp. 329–334.
64. V.V. Stegailov et al., *Shock Compression of Condensed Matter-2007* (College Park, MD: American Physical Society, 2008), pp. 339–342.
65. G.W. Nieman, J.R. Weertman, and R.W. Siegel, *J. Materials Research*, 6 (1991), pp. 1012–1027.
66. J. Shiøtz, F.D. Di Zolla, and K.W. Jacobsen, *Nature*, 391 (1998), p. 561.
67. W.G. Woifler, *Philos. Mag. A*, 58 (1988), p. 285.

Marc A. Meyers, Sirirat Traiviratana, V.A. Lubarda, and David J. Benson are with the Department of Mechanical and Aerospace Engineering, and Meyers is also with the Department of Nanoengineering, Materials Science and Engineering Program, University of California, San Diego, La Jolla, CA 92093. Eduardo M. Bringa is with Instituto de Ciencias Basicas, Universidad Nacional de Cuyo, Mendoza, Argentina. Dr. Meyers can be reached at mameyers@ucsd.edu.